Chondroblastoma and chondromyxoid fibroma: disentangling the neoplastic chondrogenesis of two rare cartilaginous tumours

Salvatore, R.

Chapter 5

TGF-β1 drives partial myofibroblastic differentiation in chondromyxoid fibroma of bone.

Salvatore Romeo[1], Brian Eyden[2], Frans A Prins[1], Inge H Briaire-de Bruijn[1], Antonie H.M. Taminiau[3], Pancras C.W. Hogendoorn[1]

Departments of Pathology[1] and Orthopaedic Surgery[3], Leiden University Medical Center, Leiden, The Netherlands; Department of

J Pathol. 2006; 285:26-34

Abstract
Chondromyxoid fibroma (CMF) is a rare benign cartilaginous bone tumor with a lobular architecture containing stellate and myofibroblast-like spindle cells. The aim of this study was to investigate the presence, spatial distribution and extent of myoid differentiation in CMF and to evaluate a possible causative role of TGF-β1 signaling, which is known to promote smooth muscle actin (SMA) expression.
Twenty cases were studied for immunoreactivity for muscle specific actin (MSA), SMA, desmin, h-caldesmon, calponin, TGF-β1 and PAI-1. The extent of myofibroblastic differentiation was further investigated ultrastructurally, including immuno-electron microscopy using antibodies against MSA and SMA, focussing upon the different cell types in CMF. The expression of potential genes driving this process was quantified by Q-PCR (TGF-β1, fibronectin, its EDA splice variant and PAI-1). Tumor cells, especially those with a spindled morphology, showed diffuse immunoreactivity for MSA, SMA, TGF-β1 and PAI-1, while desmin, h-caldesmon and calponin were absent. Ultrastructurally, neoplastic cells showed the presence of myofilaments and rare dense bodies, which were more prominent in spindle cells and less so in chondroblast-like cells. Immuno-electron microscopy confirmed the actin nature of these myofilaments. No fibronexus was identified. The functional activity of TGF-β1 was demonstrated by
the identification of PAI-1, a related downstream molecule both immunohistochemically as well as by Q-PCR. There was a linear correlation between TGF-β1 and PAI-1 expression. Fibronectin-EDA levels were low.
We substantiated the presence of morphological, immunohistochemical and immuno-electronmicroscopical partial myofibroblastic differentiation in CMF, driven by TGF-β1 signalling.

Introduction

Chondromyxoid fibroma (CMF) is a rare neoplasm of bone occurring with a diverse spectrum of age and anatomical site.[1-4] Histologically, CMF is characterised by lobules of myxoid/chondroid matrix rimmed by spindle cells often admixed with multinucleated giant cells. These morphological features are wider than that observed in mature hyaline cartilage and probably resemble the differentiation potential of cartilaginous cells *in vivo* and *in vitro.*[5,6]

There are scattered reports of SMA expression as well as ultrastructural evidence of myofilaments with focal densities in cartilaginous neoplasms.[7-9] In CMF, this was particularly reported in the spindle cell areas in a small series of cases.[8] However, the spectrum and nature of myoid/myofibroblastic differentiation of the neoplastic cells was not studied in depth.[8] Furthermore, insight into the molecular mechanism driving this cellular plasticity is lacking.

It has been shown that articular cartilage cells may show contractile function and smooth-muscle actin (SMA) expression.[10-12] The latter can be upregulated by TGF-β1 or downregulate by platelet derived growth factor BB (PDGF-BB).[12] In particular *de novo* SMA expression under TGF-β induction is a well known part of the process of transdifferentiation of fibroblasts towards myofibroblasts.[13-15] The myofibroblast has been characterized by the following parameters: a spindle-cell morphology; frequently a collagenised matrix; an immunophenotype of vimentin, SMA, MSA, calponin, desmin (mostly in lesional but not reactive myofibroblasts) and negativity for h-caldesmon.[15,16] Ultrastructurally prominent rER, modestly developed and mainly peripheral bundles of myofilaments with focal densities, and fibronexus junctions are found. The latter has been argued as a good ultrastructural marker for the myofibroblast.[15,17] A major component of the fibrils of the fibronexus is the EDA splice variant of FN (FN)[13], the expression of this splice variant being strictly regulated by TGF-β signalling.[13,18]

This *in vivo* study aims to define the extent of myofibroblastic differentiation in CMF and to test a possible causative role for TGF-β1 signalling. For this purpose an extensive array of techniques was used: conventional immunohistochemistry, reflection contrast microcopy as well as (immuno-) electron microscopy, whereas the key molecules were further quantified by Q-PCR. The *in vivo* activity of TGF-β was tested through the evaluation of PAI-1 expression in tumor cells.[19-23]

Materials and methods

Clinico-pathological data and procedures

Twenty specimens (Table 1) were retrieved from the surgical pathology files of the Leiden University Medical Center and the registry of the Netherlands Committee on Bone Tumors. One case (#20) was kindly provided by the Department of Pathology of Ghent University. Clinical information was obtained from patients' notes. All patient material was coded, such that code breaking and correlation with clinical data were only possible for physicians involved in treatment of the patients. The subsequent research was conducted following the ethical guidelines of the National organization of scientific societies (FEDERA). The 20 specimens consisted of 18 primary tumors and the recurrence from each of cases 3 and 7. The specimens were formalin-fixed, treated with formic acid (pH 2.1) for decalcification, and paraffin-embedded for subsequent haematoxylin and eosin staining of histological sections and immunohistochemical analysis. All cases were reviewed histopathologically in concert with radiology, to confirm the diagnosis.

Immunohistochemistry
Immunohistochemistry was performed as previously described.[24,25] Antibodies are listed in Table 2. Appropriate parallel positive control slides were prepared according to each antibody specificity (Table 2). Internal positive controls (Table 2) were present in all the histological sections, allowing evaluation of the antigenic property of the tissue after decalcification. As negative controls, slides were incubated with mouse-, or rabbit immunoglobulin of a corresponding (iso-) type and concentration instead of primary specific antibodies. By evaluation of the internal and external positive control, the decalcification with formic acid according to our protocol has no significant influence on antigen recognition by the antibodies used.[24-28]

Electron Microscopy and Immuno-electron Microscopy
Electron microscopy was performed on two cases (# 2 and 19) as previously described.[29] Ultrathin sections were examined in a JEOL JEM-1011 electron microscope with digital photography using a MegaView III camera.
Additionally, immuno-electron microscopy for SMA and MSA was performed. In a complementary way, reflection contrast microscopy was used as a guide for immuno-electron microscopy on sequential ultra-thin sections, since it provides exact location, size, intensity and pattern of immunolabeling, and the relation to anatomical structures.[29] For both techniques, negative controls were prepared with incubation with secondary antibodies only.

mRNA expression studies
Snap frozen samples from the primary tumor were available from 6 cases (#2, 3, 11, 13,19 and 20). RNA was extracted as described[30], only after histological evaluation of the relative section, in samples in which the tumor cellularity was at least 70% of the total surface.

Quantitative PCR (Q-PCR)

One mg of total RNA was reverse transcribed with AMV Reverse Transcriptase (Roche). The Q-PCR reactions were performed on iCycler (BioRad, Hercules, CA, USA) using SYBR Green I mastermix according to the manufacturer's instructions. For each gene a calibration curve, consisting of a mixture of the samples, was included to allow calculation of relative starting quantities of each gene. All reactions were carried out in duplicate and normalized to the geometric mean of three stable reference genes (G protein-coupled receptor 108: GPR108, heterogeneous nuclear ribonucleoprotein H1: HNRPH1, calpain small subunit 1: CAPNS1).[31] The latter were selected from expression profiling experiments of enchondromas, central chondrosarcomas (different grades), normal epiphyseal growth plates, and resting cartilage samples, demonstrating the least variation between all samples.[32] We analyzed the following genes: TGF-β1, FN and PAI-1. Primers sequences are detailed in Table 3. The log10 of the normalized relative starting quantities were used in the statistical analysis. Statistical analyses were performed using R computing environment 2.01 (http://www.R-project.org).[33]

FN/FN EDA ratio

As previously described[18], cDNA was prepared using AMV reverse transcriptase RT (Roche, Germany), according to the manufacturer's instructions and PCR was performed. Primers flanking the EDA region were used so that 526 bp amplification product corresponded to FN mRNA, which included the EDA region, while the 256 bp product corresponded to EDA-negative FN mRNA. DNA fragments were analysed by electrophoresis and the radioactivity of each PCR product was visualized with a Phosphor Imager 445 SI (Molecular Dynamics, Sunnyvale, CA). The ratio between the two was calculated as the percentage of the splice variant versus the total FN. Primers are given in table 3.

Table 1: Clinicopathological data

Case	Gender	Age	Bone
1.	M	20	femur
2.	M	14	thumb
3.	M	15	metatarsus
4.	M	49	tibia
5.	M	16	metatarsus
6.	F	34	ulna
7.	M	8	tibia
8.	M	7	femur
9.	F	60	os ilium
10.	F	35	tibia
11.	F	10	metatarsus
12.	M	15	tibia
13.	M	63	tibia
14.	F	9	tibia
15.	M	27	metatarsus
16.	F	29	os ilium
17.	M	23	femur
18.	F	41	rib
19.	M	39	sternum
20.	F	12	femur

Table 2: Details of antibodies

Antigen	Clone	Source	Species	Positive control	Dilution	Antigen retrieval
Caldesmon	h-Cald	Neomarkers	M	colon	1:500	citrate MW/10m
Calponin	Calp	Neomarkers	M	breast carcinoma	1:3000	citrate MW /10m
Desmin	cl.33	Pathol-az	M	colon	1:400	no
MSA	HHF-35	Dako	M	colon	1:1000	no
SMA	ASM-1	Progen	M	colon	1:2000	no
TGFβ1	SP208	Pathol-az	R	breast carcinoma	1:800	citrate MW /10m
PAI-1		American diagnostica inc	M	breast carcinoma	1:500	no

Legend of abbreviations: muscle specific actin: MSA; smooth muscle actin: SMA; plasminogen activator inhibitor type 1: PAI-1; mouse: M; rabbit: R; MW: microwave oven

Table 3: Sequences of the primers used for mRNA expression studies

Gene	Accession Number	Forward primer	Reverse primer
TGF-β1 [41]	NM_000660	cccagcatctgcaaagctc	gtcaatgtacagctgccgca
FN [42]	NM_212482	ggagaattcaagtgtgaccctca	aggcaacgtgttacgatgatgggaagacat
FN/FN EDA [43]	NM_212482	aaacagaaatgactattgaaggcttg	agagcatagacactcaacttcatattt
PAI1 [44]	NM_000602	cctgggaatgaccgacatgt	tgcgggctgagactagaca
GPR108	XM_290854	agatgccccttttcaagctctac	gccatgagccagtggatcttg
HNRPH1	NM_005520	gatgtagcaaggaagaaattgttcag	caccggcaatgttatcccat
CAPNS1	NM_001749	atggttttggcattgacacatg	gcttgcctgtggtgtcgc

Results

Light microscopy

All cases fitted the clinico-radiological and histological diagnostic criteria for chondromyxoid fibroma.[2] We observed lobules of chondromyxoid matrix rimmed by more cellular areas, mainly composed of spindle cells (Fig.1A). The two areas merged together gradually with changes in cell shape, slender in the cellular areas and round (chondroblast-like) in the cartilage-like areas. Cells with intermediate features, stellate and triangular, were interposed between the 2 areas, embedded in myxoid matrix.

Immunohistochemistry

Neoplastic cells were positive for MSA (Fig.1C-D), SMA and negative for desmin, h-caldesmon and calponin. Spindle cells were diffusely positive in all samples (Fig.1D); scanty positive chondroblast-like cells were found only in 3 cases (Fig.1C) (case 2, 19 and 20). Stellate cells were positive although less than the spindle ones. The staining intensity was moderate to high with MSA and mild to moderate for SMA. According to the lobular organization of CMF the immunostain for SMA and MSA showed a distinct localization being intense and diffuse at the periphery of the lobules, where spindle cells are present, and slowly fading towards the center of the lobule, where chondroblast-like cells are located.
Diffuse positivity for TGF-β1 (Fig.1E) and PAI-1 (Fig.1F) was recorded in all cases, both for the neoplastic cells and the nearby giant cells and normal connective tissue.

Electron microscopy and Immuno-electron microscopy

Three main cell-types were identified (main features of which are summarized in Table 4): chondroblast-like cells, spindle myofibroblast-like cells and cells with intermediate features. Chondroblast-like cells were rounded with prominent rough endoplasmic (rER) cisternae (Fig. 2C), and a few unremarkable mitochondria. Some cells were clear and lacked glycogen while others contained dense glycogen. Spindled cells had very prominent rER. Slender processes, mostly without organelles and containing myofilaments, were associated with both spindled and chondroblastoid cells. In a few cells, these tracts of filaments had focal densities of the type characterising smooth-muscle myofilaments (*dense zones, dense*

Table 4: Main features of the three type of cells observed in CMF

	Myofibroblast-like	Intermediate	Chondroblast-like
Morphology	spindle cells embedded in fibrous matrix	stellate cells embedded in myxoid matrix	round cells embedded in chondroid matrix
IHC	SMA and MSA intense and diffuse	SMA and MSA moderate and less diffuse	SMA and MSA scanty
EM	myofilaments, dense bodies, no fibronexus	rare myofilaments, no dense bodies, no fibronexus	no myofilaments no dense bodies, no fibronexus
IEM	well organized filamentous structures positive for SMA and MSA	less organized filamentous structures positive for SMA and MSA	no structure positive for SMA or MSA

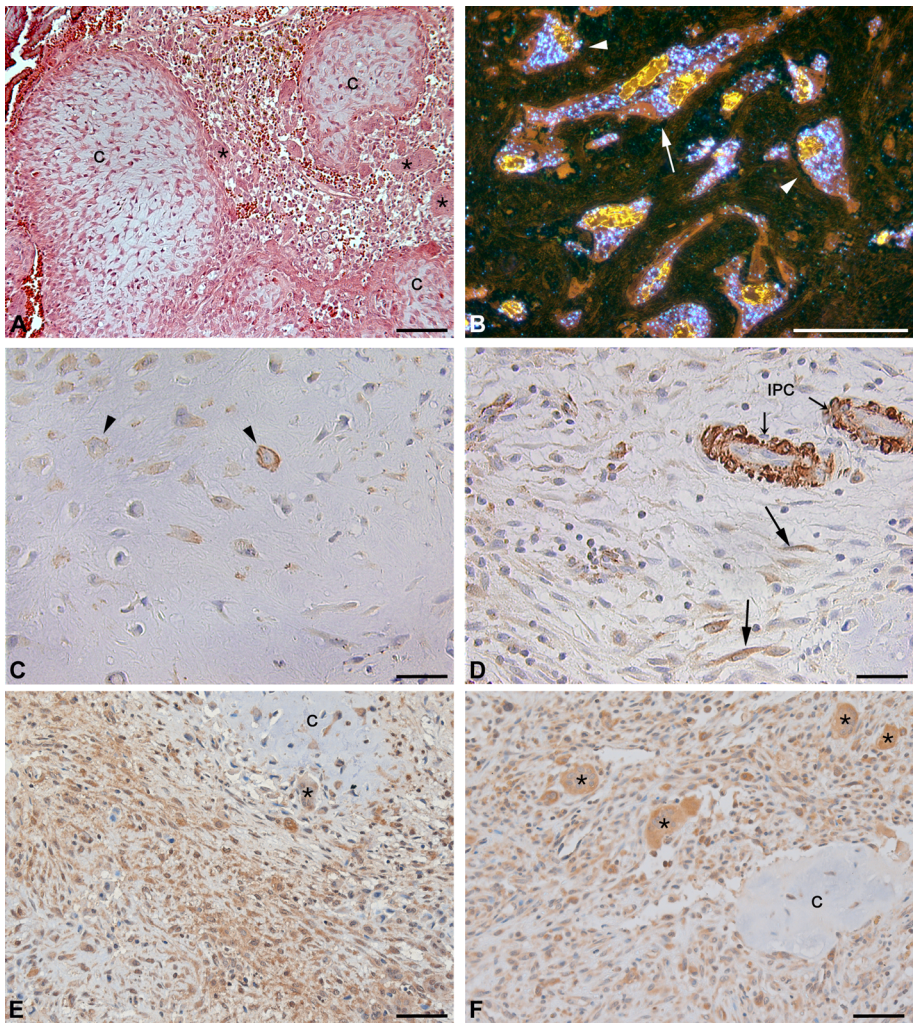

Fig.1: A) CMF is made up of lobules of spindle and stellate cells embedded in myxochondroid matrix (C); giant cells (*) are often present (10x original magnification; magnification bar: 100μm), B) reflection contrast microscopy with immunogold stain for SMA (light blue granules) showing positive spindle (arrow) and stellate (arrowhead) neoplastic cells (100x original magnification: magnification bar:10μm). C) Scant round cells (arrowhead) were positive for MSA stain (40x original magnification; magnification bar:25μm) D) Immunostaining for MSA showed diffuse positivity of the spindle cell component (arrow); intense signal on the blood vessel walls (ipc: internal positive control) confirms the preservation of antigenic properties (40x original magnification; magnification bar: 25μm). E) and F) Immunostain on consecutive slides respectively for TGF-β1 and PAI-1 showing intense signals in the same cells, both neoplastic and non-neoplastic (* indicates multinucleated giant cells) (C indicates myxochondroid lobules) (20x original magnification; magnification bar: 50μm).

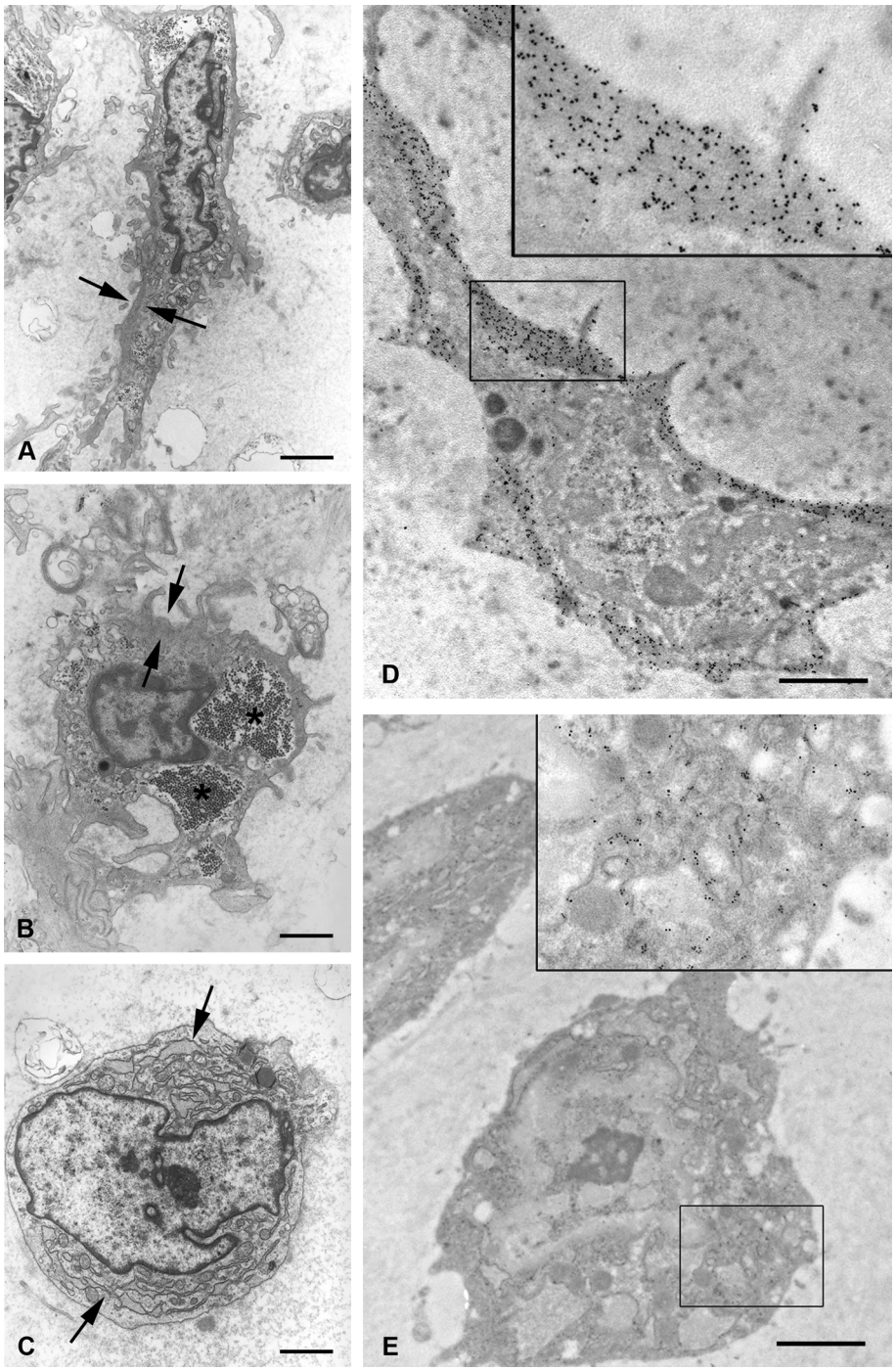
A
B
C
D
E

Fig 2: Morphological spectrum of partial myofibroblastic differentiation (A, B and C). A) Spindle cell showing subplasmalemmal myofilaments (between arrows) in the absence of fibronexuses and glycogen (*). B) Round cell with intermediate features are found with evident subplasmalemmal myofilaments (between arrows) and glycogen (*) but without fibronexuses or dense bodies. C) Round cell with chondroblastic appearance with evident rER (arrows). D and E: Immuno-electron microscopy. D) Peripheral cellular distribution of SMA immunoreactivity in a spindled cell. Inset: detail showing that the myofilaments are made up of filamentous smooth muscle actin (as shown by the accumulation by immunogold labelled particles). E) Some round cells show evidence of SMA expression but with a less well organized filamentous structure. Inset: detail of the mentioned organization of SMA depicted by immunogold particles (magnification bar: 2μm).

bodies), but these were rather uncommon. No fibronexus junctions were identified. However some cells focally had a partial coating of low-density material, reminiscent of a lamina. Cells with intermediate morphology were found. Such cells showed a stellate or round shape , myofilaments were present although less organized then in the spindle cells, no focal densities were observed

The high resolution of reflection contrast microscopy showed an intracellular presence of SMA (Fig. 1B) and MSA. Immuno-electron microscopy on consecutive sections confirmed the actin content of the ultrastructurally identified myofilaments. Positive staining for MSA and SMA was found both in spindle and round or stellate cells, although some important differences were found. In the spindle cells, filamentous structures were clearly recognizable in the background to the immuno-gold particles, while in round or stellate cells such structures were not so evident (SMA ultra-immunostains shown in Fig.2D and E). As for the immunohistochemistry, the MSA stain was somewhat more intense than the SMA stain, perhaps because of cross-reaction with different actin isotypes.

Q-PCR

TGF-β1, FN and PAI-1 were shown to be expressed at the RNA level. In particular TGF-β1 and PAI-1 levels of expression were significantly correlated (R^2:0.88 and p:0.006) as well as TGF-β1 and FN (R^2:0.81 and p: 0.01)(Fig.3), thus substantiating active TGF-β1 signalling.

FN/FN EDA ratio

The EDA splice variant of FN was expressed as 2±1.6% of the total FN (range: from 0 to 3.7%) in accordance with the presence of partial myofibroblastic differentiation.

Discussion

The observations presented here extend our knowledge and understanding of the differentiation in chondromyxoid fibroma, as well as the mechanism underlying neoplastic chondrocyte phenotypic plasticity. The terminology for this tumour stems from a baseline differentiation with similarities to cartilage, based on histological, histochemical, immunohistochemical and ultrastructural studies and the characteristic spectrum of cell types ranging from rounded chondroblastic cells to spindled, more fibroblastic elements.[2] Of particular interest in chondromyxoid fibroma, and certain other chondroblastic tumours and cartilaginous cells, is the presence of smooth-muscle elements as defined by immunohistochemistry and electron microscopy – actin immunostaining (MSA and SMA) and ultrastructurally identified myofilaments with focal densities. The focus

of discussion here is the nature and meaning of this "myoid" phenotype: 1) does it, with respect to a pre-existing or underlying cartilaginous phenotype, represent a superimposed true smooth-muscle or a myofibroblastic differentiation?2) What is the underlying mechanism driving this "myoid" differentiation?
Insights into the biology of the myofibroblast have widened its perception. Given the known transdifferentiation of fibroblast to myofibroblast, one cannot expect a rigid distinction between these two cell-types, which introduces the concept of degrees of myofibroblast differentiation, or partial myofibroblastic differentiation. In this regard, in vitro experiments have shown fibroblasts to acquire the phenotype of differentiated myofibroblasts through intermediate features of proto-myofibroblast.[14]
Previous authors recognising actin immunostaining or myofilaments in cartilaginous tumours have interpreted these findings as myofibroblastic without further qualification.[8] According to our observations, the full myofibroblastic phenotype is not achieved in chondromyxoid fibroma, since there is still recognisable cartilaginous differentiation, and there are no fibronexus junctions (Smooth-muscle transdifferentiation, incidentally, is not favoured here, because of the ultrastructural absence of plaques, caveolae and lamina, and the negative immunostaining for desmin and h-caldesmon). Consistent with the absence of fibronexuses and our view of partial myofibroblastic transdifferentiation in CMF, we showed m-RNA expression for FN with low or absent expression of its ED-A splice variant.
One of the principal differences, then, between fibroblasts and myofibroblasts is the absence of SMA and myofilaments in fibroblasts and their presence in the myofibroblast. Results from a variety of sources suggest that the primary mechanism for the de novo synthesis of SMA involves TGF-β.[14] Our findings are the first demonstration of TGF-β in this tumour. In particular, the present study not only demonstrated the presence of TGF-β1 both at the protein and mRNA expression level but proved its activity, too. Since TGF-β protein is released as an inactive 'latent' complex.[4] The activity of TGF-β1 was assessed through protein and m-RNA expression of the downstream molecule, PAI-1. In fact TGF-β1 is known to down-regulate the expression of ECM-degrading proteases and induces proteinase inhibitors like PAI-1and tissue inhibitor of metalloproteinase-1, both in vitro as well as in vivo.[20,35,36]
We demonstrated a diffuse and intense signal for PAI-1 protein in CMF, with a localization overlapping with that of TGF-β1, both in neoplastic cells as well as in the nearby normal connective tissue and in the giant cells. Furthermore, we showed PAI-1 m-RNA expression to significantly correlate with levels of TGF-β1 confirming the activity of TGF-β1 in inducing PAI-1 expression. This is striking, especially considering that several other signalling molecules are known to upregulate PAI-1 expression. As a further proof of the activity of TGF-β1, we also found a positive significant correlation with FN expression, for which, as for most of the extracellular matrix components, TGF-β is known to exert a stimulatory effect.[37,38]
We have demonstrated immunohistochemically, ultrastructurally and immuno-ultrastructurally the presence in chondromyxoid fibroma neoplastic cells of myofilaments with rare focal densities, containing SMA and MSA. Immuno-ultrastructural analysis showed few round or stellate cells positive for SMA and MSA. In the round cells with more chondrocytic features, filamentous structures are not clearly recognizable. Since actin molecules can be present in the cytoplasm as globular monomers and polymerize to form filaments, this result probably reflects

the different organizational status of the actin molecules. Hence the morphological spectrum of differentiation from myofibroblast-like spindle cells to chondrocyte-like cells might be reflected in a different level of molecular organization of these contractile structures. It is difficult to know the dynamics of this differential expression of actin: are there factors in chondrocyte-like cells preventing polymerization of actin monomers? Or, do polymerised actin filaments in chondrocyte-like cells degrade to give rise to actin-depleted cells? Such hypotheses require further study. However, these observations are collectively strikingly similar to an in vitro and in vivo articular chondrocyte model, where the SMA positive cells are slender and at the surface of articular cartilage, or at the periphery of 3-dimensional cultures.[10-12] Probably the different distribution and consequently the probable different organization of the contractile proteins reflect a different functionality in terms of ability to contract the nearby extracellular matrix. It is likely to predict that a slender cell would be more prone to contraction than a round one. Conversely, as reported in the literature, the round cells are more efficient in producing aggrecan and collagen type II, while the spindle cells produce mainly collagen type.[39]

Hence our in vivo observations prompt a model of paracrine and autocrine TGF-b1 signalling, between neoplastic and non-neoplastic stromal cells (Fig. 4A), for which we have clearly proved the activity, promoting a different organization of the contractile actin in spindle and round cells, with a continuous spectrum (Fig. 4B), and in parallel a different production of extracellular matrix. TGF-b1 is ubiquitously expressed in tissue of mesodermal origin, and in particular in cartilaginous cells is also known to induce specific extracellular matrix production according to the state of differentiation and the organization of the actin cytoskeleton.[40] The proposed model takes in account both the actual knowledge on chondrogenesis as well as our in vivo observations. Eventual in vitro experimentation on CMF could be of further help. However, the rarity of CMF and the difficulty to culture primary tumour cells are obstacles to such experiments.

In conclusion, chondromyxoid fibroma shows an early stage of myofibroblastic differentiation superimposed, via a partial transdifferentiation process, on to an underlying cartilaginous phenotype. This is consistent with absence of desmin and h-caldesmon staining, and the absence of cell-surface plaques, caveolae and lamina, all of which would indicate a smooth-muscle type of differentiation. The absence of fibronexus is also consistent with this partial myofibroblastic phenotype. We have shown immunohistochemically, ultrastructurally and immuno-ultrastructurally evidence of different degrees of partial myofibroblastic differentiation amongst stellate and chondroblast-like cells. Our results on TGF-b1 and related downstream molecules strongly suggest this molecule as a causative agent in driving partial myofibroblastic differentiation in cartilaginous tumours such as chondromyxoid fibroma.

Acknowledgements

We would like to acknowledge Dr. R. Forsyth for the case from Ghent University, M. Eikmans PhD, E. de Heer PhD and A. Gorter PhD for critical discussion, J. Ooosting for the bioinformatics expertise and L. Hameetman, MSc, J.J. Baelde and K. Philippo for expert technical help. Part of the data was presented to USCAP 2005.

Reference List

1. Gherlinzoni F, Rock M, Picci P. Chondromyxoid fibroma. The experience at the Istituto Ortopedico Rizzoli. J Bone Joint Surg [Am] 1983; 65:198-204.
2. Ostrowski ML, Spjut HJ, Bridge JA. Chondromyxoid fibroma. In: Fletcher CDM, Unni KK, Mertens F, editors. World Health Organization classification of tumours. Pathology and genetics of tumours of soft tissue and bone. Lyon: IARC Press, 2002: 243-245.
3. Schajowicz F, Gallardo H. Chondromyxoid fibroma (fibromyxoid chondroma) of bone. A clinico- pathological study of thirty-two cases. J Bone Joint Surg Br 1971; 53(2):198-216.
4. Zillmer DA, Dorfman HD. Chondromyxoid fibroma of bone: thirty-six cases with clinicopathologic correlation. Hum Pathol 1989; 20:952-964.
5. Cancedda R, Descalzi CF, Castagnola P. Chondrocyte differentiation. Int Rev Cytol 1995; 159:265-358.
6. Romeo S, Bovée JVMG, Grogan S, Taminiau AHM, Eilers PHC, Cleton-Jansen AM et al. Chondromyxoid fibroma resembles in vitro chondrogenesis, though differs in expression of signalling molecules. J Pathol 2005; J Pathol. 206:135-142.
7. Hasegawa T, Seki K, Yang P, Hirose T, Hizawa K, Wada T et al. Differentiation and proliferative activity in benign and malignant cartilage tumors of bone. Hum Pathol 1995; 26:838-845.
8. Nielsen GP, Keel SB, Dickersin GR, Selig MK, Bhan AK, Rosenberg AE. Chondromyxoid fibroma: a tumor showing myofibroblastic, myochondroblastic, and chondrocytic differentiation. Mod Pathol 1999; 12(5):514-517.
9. Povysil C, Tomanova R, Matejovsky Z. Muscle-specific actin expression in chondroblastomas. Hum Pathol 1997; 28(3):316-320.
10. Kim AC, Spector M. Distribution of chondrocytes containing alpha-smooth muscle actin in human articular cartilage. J Orthop Res 2000; 18(5):749-755.
11. Kinner B, Spector M. Smooth muscle actin expression by human articular chondrocytes and their contraction of a collagen-glycosaminoglycan matrix in vitro. J Orthop Res 2001; 19(2):233-241.
12. Zaleskas JM, Kinner B, Freyman TM, Yannas IV, Gibson LJ, Spector M. Growth factor regulation of smooth muscle actin expression and contraction of human articular chondrocytes and meniscal cells in a collagen-GAG matrix. Exp Cell Res 2001; 270(1):21-31.
13. Dugina V, Fontao L, Chaponnier C, Vasiliev J, Gabbiani G. Focal adhesion features during myofibroblastic differentiation are controlled by intracellular and extracellular factors. J Cell Sci 2001; 114(Pt 18):3285-3296.
14. Gabbiani G. The myofibroblast in wound healing and fibrocontractive diseases. J Pathol 2003; 200(4):500-503.
15. Eyden B. The myofibroblast: an assessment of controversial issues and a definition useful in diagnosis and research. Ultrastruct Pathol 2001; 25(1):39-50.
16. Watanabe K, Kusakabe T, Hoshi N, Saito A, Suzuki T. h-Caldesmon in leiomyosarcoma and tumors with smooth muscle cell-like differentiation: its specific expression in the smooth muscle cell tumor. Hum Pathol 1999; 30(4):392-396.
17. Eyden BP. Brief review of the fibronexus and its significance for myofibroblastic differentiation and tumor diagnosis. Ultrastruct Pathol 1993; 17(6):611-622.
18. Baelde HJ, Eikmans M, van Vliet AI, Bergijk EC, De Heer E, Bruijn JA. Alternatively spliced isoforms of fibronectin in immune-mediated glomerulosclerosis: the role of TGFbeta and IL-4. J Pathol 2004; 204(3):248-257.
19. Hazelbag S, Gorter A, Kenter GG, van den BL, Fleuren G. Transforming growth factor-beta1 induces tumor stroma and reduces tumor infiltrate in cervical cancer. Hum Pathol 2002; 33(12):1193-1199.
20. Pasini FS, Brentani MM, Kowalski LP, Federico MH. Transforming growth factor beta1, urokinase-type plasminogen activator and plasminogen activator inhibitor-1 mRNA expression in head and neck squamous carcinoma and normal adjacent mucosa. Head Neck 2001; 23(9):725-732.

21. Alessi MC, Bastelica D, Morange P, Berthet B, Leduc I, Verdier M et al. Plasmin ogen activator inhibitor 1, transforming growth factor-beta1, and BMI are closely associated in human adipose tissue during morbid obesity. Diabetes 2000; 49(8):1374-1380.
22. Dong C, Zhu S, Yoon W, Wang T, Alvarez RJ, Goldschmidt-Clermont PJ. Upregulation of PAI-1 is mediated through TGF beta /SMAD pathway in transplant arteriopathy. J Heart Lung Transplant 2001; 20(2):219.
23. Dong C, Zhu S, Wang T, Yoon W, Li Z, Alvarez RJ et al. Deficient Smad7 expression: a putative molecular defect in scleroderma. Proc Natl Acad Sci U S A 2002; 99(6):3908-3913.
24. Romeo S, Bovée JVMG, Jadnanansing NAA, Taminiau AHM, Hogendoorn PCW. Expression of cartilage growth plate signalling molecules in chondroblastoma. J Pathol 2004; 202(1):113-120.
25. Bovée JVMG, Van den Broek LJCM, Cleton-Jansen AM, Hogendoorn PCW. Up-regulation of PTHrP and Bcl-2 expression characterizes the progression of osteochondroma towards peripheral chondrosarcoma and is a late event in central chondrosarcoma. Lab Invest 2000; 80:1925-1933.
26. Annels NE, Da Costa CE, Prins FA, Willemze A, Hogendoorn PCW, Egeler RM. Aberrant chemokine receptor expression and chemokine production by Langerhans cells underlies the pathogenesis of Langerhans cell histiocytosis. J Exp Med 2003; 197(10):1385-1390.
27. Bovée JVMG, Van den Broek LJCM, De Boer WI, Hogendoorn PCW. Expression of growth factors and their receptors in adamantinoma of long bones and the implications for its histogenesis. J Pathol 1998; 184:24-30.
28. Lindeman JH, Hanemaaijer R, Mulder A, Dijkstra PD, Szuhai K, Bromme D et al. Cathepsin K is the principal protease in giant cell tumor of bone. Am J Pathol 2004; 165(2):593-600.
29. Prins FA, Diemen-Steenvoorde R, Bonnet J, Cornelese-ten Velde I. Reflection contrast microscopy of ultrathin sections in immunocytochemical localization studies: a versatile technique bridging electron microscopy with light microscopy. Histochem 1993; 99(6):417-425.
30. Baelde HJ, Cleton-Jansen AM, van Beerendonk H, Namba M, Bovée JVMG, Hogen doorn PCW. High quality RNA isolation from tumours with low cellularity and high extracellular matrix component for cDNA microarrays: application to chondrosarcoma. J Clin Pathol 2001; 54(10):778-782.
31. Vandesompele J, De Preter K, Pattyn F, Poppe B, Van Roy N, De Paepe A et al. Accurate normalization of real-time quantitative RT-PCR data by geometric averaging of multiple internal control genes. Genome Biol 2002; 3(7): research0034.1-0034.11.
32. Rozeman LB, Hameetman L, van Wezel T, Taminiau AHM, Cleton-Jansen AM, Hogendoorn PCW et al. cDNA expression profiling of central chondrosarcomas: Ollier disease resembles solitary tumors and alteration in genes coding for energy metabolism with increasing grade. submitted 2005.
33. R Development Core Team. R: A language and environment for statistical computing. Vienna, Austria: 2004.
34. Derynck R, Akhurst RJ, Balmain A. TGF-beta signaling in tumor suppression and cancer progression. Nat Genet 2001; 29(2):117-129.
35. Dennler S, Itoh S, Vivien D, ten Dijke P, Huet S, Gauthier JM. Direct binding of Smad3 and Smad4 to critical TGF beta-inducible elements in the promoter of human plasminogen activator inhibitor-type 1 gene. EMBO J 1998; 17(11):3091-3100.
36. Song CZ, Siok TE, Gelehrter TD. Smad4/DPC4 and Smad3 mediate transforming growth factor-beta (TGF-beta) signaling through direct binding to a novel TGF-beta-responsive element in the human plasminogen activator inhibitor-1 promoter. J Biol Chem 1998; 273(45):29287-29290.
37. Burger A, Wagner C, Viedt C, Reis B, Hug F, Hansch GM. Fibronectin synthesis by human tubular epithelial cells in culture: effects of PDGF and TGF-beta on synthesis and splicing. Kidney Int 1998; 54(2):407-415.

38. Lam S, Verhagen NA, Strutz F, van der Pijl JW, Daha MR, van Kooten C. Glucose-induced fibronectin and collagen type III expression in renal fibroblasts can occur independent of TGF-beta1. Kidney Int 2003; 63(3):878-888.
39. Soder S, Inwards C, Muller S, Kirchner T, Aigner T. Cell biology and matrix biochemistry of chondromyxoid fibroma. Am J Clin Pathol 2001; 116(2):271-277.
40. Jakob M, Demarteau O, Schafer D, Hintermann B, Dick W, Heberer M et al. Specific growth factors during the expansion and redifferentiation of adult human articular chondrocytes enhance chondrogenesis and cartilaginous tissue formation in vitro. J Cell Biochem 2001; 81(2):368-377.